

## Ceramics by Niculoso Pisano and quantitative analysis of glazes using portable XRF

Auxiliadora Gómez Morón **01** | Ángel Jesús Polvorinos del Río **01** | Jacques Castaing **02** | Alfonso Pleguezuelo **03**

Chemical and mineralogical analysis has been performed on two ceramics tiles covered with coloured glazes and attributed to Niculoso Pisano. We have determined the mineralogical and chemical compositions of the bodies as well as of the different glazes, including microstructural observations of the glaze colors used in the decoration. Such ceramic composition study aims at improving the knowledge of the materials and techniques used by this artist, as well as to clarify the possible existence of various steps in the chronology of his production. In order to check for a method to achieve quantitative non-destructive characterization for art-works that cannot be moved to a laboratory, we have determined the concentrations of the elements in the different glaze colours using a portable X-ray fluorescence (PXRF) and we have compared the values to those obtained with a commercial  $\mu$ -XRF at the same places on the objects. Complementing PXRF with portable Raman spectrometry provides valuable information on ceramics similar to laboratory equipment.

### Keywords

Tile by Artist | Ceramic | Portable X-Ray Fluorescence | Electron Microscopy | Niculoso Pisano, Francisco (145?-1529?) | Renaissance (Style) | Seville (Seville) | Glazing |

## Cerámicas de Niculoso Pisano y análisis cuantitativo de vidriados por FRX portátil

Auxiliadora Gómez Morón **01** | Ángel Jesús Polvorinos del Río **01** | Jacques Castaing **02** | Alfonso Pleguezuelo **03**

En este trabajo se aborda la caracterización química y mineralógica de dos piezas cerámicas esmaltadas atribuidas a Niculoso Pisano. Se han estudiado tanto la mineralogía y composición química de las pastas cerámicas, como la caracterización química-mineralógica y microestructural de los pigmentos utilizados en la decoración de los esmaltes. El análisis de las composiciones y de su variabilidad pretende contribuir a mejorar el conocimiento científico de los materiales y técnicas utilizados por este artista, así como a dilucidar posibles indicadores de la cronología de su producción cerámica. Con el objeto de establecer un procedimiento que permita la caracterización cuantitativa por métodos no destructivos de obras cuyo análisis por técnicas convencionales no es posible, se han determinado las concentraciones de los elementos químicos de los distintos colores de los vidriados utilizando un equipo portátil de fluorescencia de rayos X (FRXP), y los resultados se comparan con los obtenidos en los mismos objetos por  $\mu$ -FRX de laboratorio. Combinando FRXP y espectrometría Raman portátiles se consigue información sobre las obras equivalente a la conseguida con equipos de laboratorio.

### Palabras claves

Azulejo de artista | Cerámica | Fluorescencia de rayos X portátil | Microscopía electrónica | Niculoso Pisano, Francisco (145?-1529?) | Renacimiento (Estilo) | Sevilla (Sevilla) | Vidriado |

URL <<http://www.iaph.es/phinvestigacion/index.php/phinvestigacion/article/view/137>>

## INTRODUCTION

Niculoso Francisco, called Pisano, a renowned tile-manufacturing master established in Seville during the late 15th century, is the most well-known ceramist –if not one of the only ones– from that time period in Spain (DAVILLIER, 1856; GESTOSO Y PÉREZ, 1903; MORALES, 1977; RAY, 1999). Two pieces of work must be highlighted from this artist's extensive portfolio: the altarpiece of the Visitación that Niculoso made for the chapel of Queen Isabella the Catholic (in the Royal Alcázar of Seville), and the altarpiece of Our Lady of Tentudía in the monastery by this same name in Segura de León (Badajoz). These pieces were dated and signed in 1504 and 1518, respectively.

Despite the breadth of his collection, unfortunately there is no analytical data on the enamels used by Pisano (PLEGUEZUELO, 2009); thus, this study focuses on the analysis of two ceramic tiles produced in his workshop using non-destructive techniques.

This study begins the comprehensive characterisation of this artist's work in ceramics, not only to determine the chemical composition and the nature of the pigments utilised, but also to detect possible evolutions in this aspect of his professional activity and to possibly authenticate works that are attributed to him.

Although taking micro-samples for their analysis using conventional laboratory techniques was possible in the case of the pieces studied, two portable non-destructive analysis techniques were applied – specifically portable X-ray fluorescence (PXRF) and portable Raman spectroscopy– in order to validate and demonstrate their usefulness for the study of other works whose importance and location make conventional laboratory analyses impossible. Validation of the data produced by the aforementioned portable non-destructive techniques was carried out by comparing it to data obtained with conventional laboratory techniques, specifically X-ray diffraction, scanning electron microscopy with energy dispersive X-ray microanalysis (EDXMA) and X-ray microfluorescence.

## DESCRIPTION OF THE PIECES STUDIED

The two tiles studied, which we will hereinafter reference as Nic1 and Nic2, are presented in images 1 and 2 respectively, showing the points on the enamels which have been analysed with both PXRF and X-ray microfluorescence ( $\mu$ -XRF) in the laboratory. Both tiles belong to a private collection in Seville (Spain) and, after analysing their formal characteristics, can be confidently attributed to the production of the aforementioned ceramist.

Nic1 is a square tile that must have formed part of a border with plant spirals of the Roman tradition which Niculoso would have learnt in Italy, where this classic repertoire had grown popular, and used in several of his pieces made in Seville. The drawing was produced using a paint brush with blue enamel and was coloured in with this same colour, green, yellow and purple. The plant motifs stand out in certain areas against the blue and purple backgrounds. The shading was created using a more diluted blue watercolour and parallel lines. The concentric arrangement of the branches and their gradually decreasing thickness as they approach the centre may indicate that the complete motif was a classic spiral volute contrasting against a purple background, while the outer background is covered in dark blue. We do not know which motif could have occupied the centre of this volute; perhaps a flower or the figure of a prodigy or a prophet. Its non-repetitive nature and the mastery evident in the brush strokes allow us to assume that this tile was produced by Niculoso's own hand.

Nic2, on the contrary, is a fragment from another square tile whose paste, size, drawing, colouring and texture fully identify with one of the motifs used on the altar of the Visitación of the Royal Alcázar. Specifically, it is associated with the stars and interweaving lines that adorn the sides of the altar table of the aforementioned altarpiece (PLEGUEZUELO, 2012). While this altar table is not missing any tiles, there are several tiles that, like this one, are kept in private collections; we should thus consider the fact that these tiles must have been employed in one of Niculoso's other pieces, such as the baseboard that has disappeared from Queen Isabella's chapel itself, or the altar table of the altarpiece that has disappeared from King Ferdinand of Aragon's chapel. The mass production of the motif allows us to imagine that the tiles were produced by skilled workers. If we associated them with similar examples from the aforementioned altarpiece they would date back, like the altarpiece, to 1504.

The manufacturing technique for both tiles can be considered standard for the time period, with slabs of clay made by filling a tile mould; that is, a simple structure or wooden frame of the desired thickness of the tile.

After being filled with clay, any extra would be removed and the rest would be smoothed out. After the clay was dried and fired it would then be soaked in white, tin-based enamel, painted with paint brushes using the colouring pigments and then fired once again. The oven needed to fire this type of piece twice is assumed to be of the Arab type, like the oven in Niculoso's workshop which was excavated in Triana in 1987, revealing pieces produced with this technique (LORENZO; VERA; ESCUDERO, 1990; PLEGUEZUELO, 1992). The dimensions of the two tiles are the same: 13cmx13cmx24mm.

The manufacturing of the tiles reveals a certain rustic nature that is detected, for instance, in the irregular texture of the decorated surface, as well as in the marks from the typical earthenware tripods which were used in Mudéjar workshops, therefore leaving visible marks when they were pulled out.

The range of colours that Niculoso brought to Seville at the end of the 15th century –and that practically disappeared following his death in 1529 or, at most, the death of his son– includes five pure colours, in addition to white (PLEGUEZUELO, 2009).

As is usual practice for this type of ceramic, the piece's white enamel was created using tin-opacified, plumbo-alkaline fritted glass. The starting materials are: silica sands, Pb compounds and alkalis as fluxes and Sn oxide (cassiterite); for its preparation, the aforementioned fritted mix was ground and, after being dispersed in water and homogenised, applied to the surface of the fired clay. The opacity of the white surface produced after the ceramic piece is fired for a second time depends on the types, sizes and abundance of the inclusions present in the glaze, as these inclusions determine the absorption and spread of light of the layer of enamel. The addition of different transition metals such as cobalt (Co), copper (Cu), iron (Fe) or manganese (Mn) into transparent fritted glass by means of minerals –generally processed– or synthesized compounds are the basis for preparation of the pigments utilised for decoration, although the final colour of the enamel will not only depend on the oxidation state, but also on the type of glass it is integrated into.

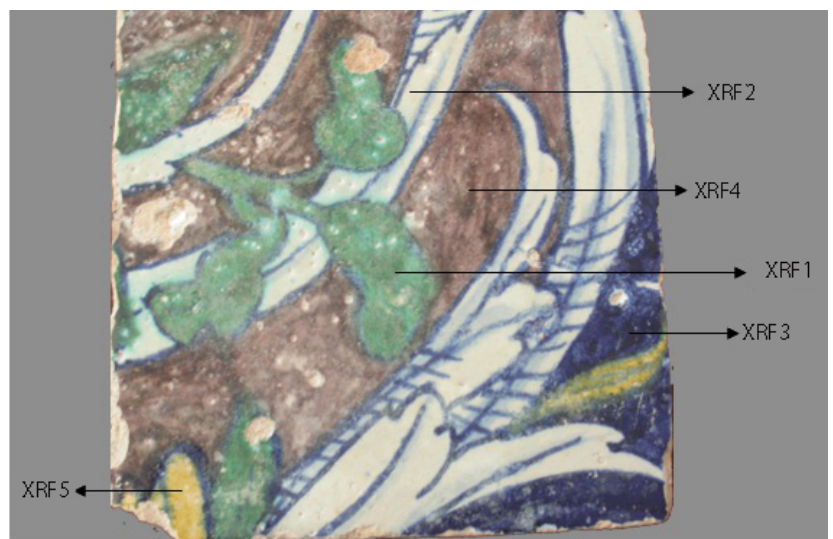


**Image 1 |**

Nic1 tile with indications showing the spots analysed with portable XRF (PXRF) and microfluorescence ( $\mu$ -XRF)

The dark blue used by Pisano to make the lines for the drawings, and the blue diluted into lighter blue tones for creating the effect of volume, is an artificial pigment which was typical at that time: blue enamel obtained by adding small amounts of Co to a transparent glass, by means of complex Co, nickel (Ni) and Fe arsenides and/or sulfides, such as skutterudite ( $\text{CoAs}_3$ ), erythrite ( $\text{Co}_3\text{As}_2\text{O}_8 \cdot 8\text{H}_2\text{O}$ ), siegenite  $(\text{Ni},\text{Co})_3\text{S}_4$ , cobaltite ( $\text{CoAsS}$ ), etc. which have been previously roasted. This type of pigment was frequently used during the entire Renaissance in both Spanish and Italian ceramics (GRATUZE; SOULIER; BLET et al., 1996; SENDOVA; ZHELYASKOV; SCALERA et al., 2007; POLVORINOS; AUCOUTURIER; BOUQUILLON et al., 2011) and different types of Co ores have been proposed as temporary distinguishing features in certain ceramic production processes (ZUCCHIATTI; BOUQUILLON; KATONA et al., 2006; ZUCCHIATTI; BOUQUILLON, 2011). Other colours suggest the use of classic formulas based on Cu for green, or on Mn for the production of browns. The use of Fe was typical during this time period for the production of yellow and beige; however, lead antimonates (Naples yellow) also appear with peculiar compositions and have been the subject of a more detailed study with the aim of characterising their specificity.

## EXPERIMENTAL ANALYSIS METHODS

Analysis of the chemical and mineralogical composition of the ceramic pastes was conducted with conventional XRF and X-ray diffraction using the powder method with samples from each ceramic fragment.

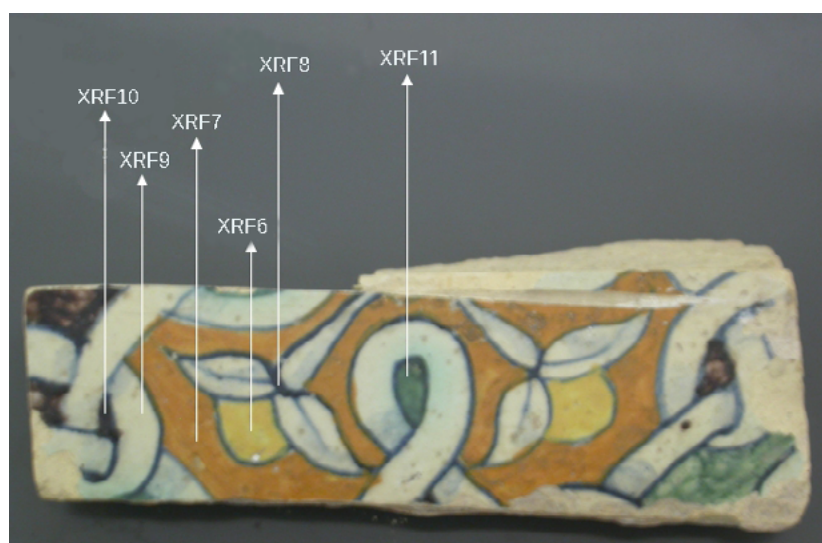


**Image 2 |** Nic2 tile with indications showing the spots analysed with portable XRF (PXRF) and microfluorescence ( $\mu$ -XRF)

Chemical analysis of each ceramic paste was carried out with a Panalytical XRF device (AXIOS model) with a tube of Rh, including an automatic sampler, 8 analysing crystals and 3 collimators. The powder samples were passed through a 50- $\mu\text{m}$  sieve and dried in an oven for 24 hours at 105 °C; 0.8 g of the sample and 4.7 g of  $\text{Li}_2\text{B}_4\text{O}_7$  were processed in order to obtain cast beads by using a Philips Perlx'2 machine with radio frequency induction. Conventional procedures were utilised to determine the concentrations of major elements ( $\text{SiO}_2$ ,  $\text{Al}_2\text{O}_3$ ,  $\text{Fe}_2\text{O}_3$ ,  $\text{MgO}$ ,  $\text{CaO}$ ,  $\text{Na}_2\text{O}$ ,  $\text{K}_2\text{O}$ ,  $\text{TiO}_2$ ,  $\text{P}_2\text{O}_5$ ) as well as trace elements (Ba, Co, Cu, Mn, Ni, Pb, Rb, Sr, V, Zn, Zr, Nb); the concentrations presented are given in % by weight and parts per million (ppm) respectively (table 1).

Mineralogical analysis by X-ray diffraction of the ceramic pastes was carried out with a Bruker diffractometer (D8 Advance model) with a Cu tube and an Ni filter; it operates at 40 kV and 20 mA, covers between 5 and 60° and has a step size of 0.02 ° and an exposure time of 2 s/step.

The EVA programme was utilised for identification of the phases. Analysis by X-ray microdiffraction ( $\mu\text{-XRD}$ ) of the crystalline phases present in the yellow and beige glazes was conducted using a Bruker diffractometer (D8 Discover model) with a Cu tube, a precise focusing lens that integrates a polycapillary system and a double Gobel mirror, and an area detector (VANTEC-500 model).

**Table 1 |**

The concentrations of the pastes in the Nic1 and Nic2 tiles are indicated in the 2nd and 3rd columns, while the 4th column shows the variation ranges of the pastes in ceramics decorated with lustre (RFM), produced in Seville (POLVORINOS; CASTAING, 2010). The major elements and loss upon calcination (P.C.) are indicated in % and the rest of the elements in ppm

	NIC 1	NIC 2	RFM		NIC 1	NIC 2	RFM
$\text{SiO}_2$ (%)	46.2	38.7	49 ± 1.7	Mo (ppm)	2.6	2.8	
$\text{Al}_2\text{O}_3$ (%)	10.5	8.2	11.6 ± 0.4	Nb (ppm)	1.0	5.8	
$\text{Fe}_2\text{O}_3$ (%)	4.4	3.3	3.8 ± 0.24	Nd (ppm)	21.1	17.1	
MnO (%)	0.1	0.0		Ni (ppm)	45.4	17.0	
MgO (%)	3.5	2.8	3.5 ± 0.42	Pb (ppm)	363.1	309.7	
CaO (%)	21.8	22.3	22 ± 2.16	Rb (ppm)	82.2	58.4	51 ± 5
$\text{Na}_2\text{O}$ (%)	0.9	0.7	0.9 ± 0.2	Sc (ppm)	14.4	13.2	
$\text{K}_2\text{O}$ (%)	2.0	2.4	1.8 ± 0.7	Sm (ppm)	4.1	4.2	
$\text{TiO}_2$ (%)	0.5	0.4	0.5 ± 0.03	Sr (ppm)	440.6	450.4	423 ± 13
$\text{P}_2\text{O}_5$ (%)	0.1	0.2	0.2 ± 0.04	Ta (ppm)	N.D.	N.D.	
$\text{SO}_3$ (%)	0.2	0.3		Th (ppm)	10.1	13.3	
As (ppm)	44.4	13.8		Tl (ppm)	2.8	2.3	
Ba (ppm)	239.4	204.5	281 ± 33	V (ppm)	72.4	57.0	
Cl (ppm)	340.1	294.5	535 ± 141	U (ppm)	2.6	4.4	
Co (ppm)	17.2	12.4	18 ± 2	W (ppm)	5.6	11.8	
Cr (ppm)	64.8	29.6	75 ± 30	Y (ppm)	21.3	19.8	19 ± 1
Cu (ppm)	72.2	29.6	45 ± 7	Yb (ppm)	2.9	2.4	
Ga (ppm)	17.3	15.2	19 ± 3	Zn (ppm)	131.5	99.8	73 ± 7
Hf (ppm)	4.3	4.3		Zr (ppm)	167.2	157.7	
La (ppm)	22.6	20.4		P.C. (%)	8.9	19.6	

For the non-destructive quantitative analysis of the chemical composition of the different colours of glazes, an EAGLE III microbeam X-ray fluorescence ( $\mu$ -XRF) analyser was used; this device incorporates an X-ray tube with an Rh anode and a Si(Li) energy dispersive X-ray detector. It features a camera that focuses the surface of the sample using a 50  $\mu$ m-diameter X-ray beam to identify the elements that are present (Na to U) and their quantitative analysis by the fundamental parameter approach.

Other chemical composition measurements of the surface of the glazes were taken with an AMPTEK portable XRF spectrometer, using a tungsten anode X-ray tube with a maximum power of 3.6 watts at 40 kV and a current of 90  $\mu$ A; the focal spot size of the beam measures 2 mm. X-ray fluorescence measurements were taken using a Silicon Drift detector, cooled to -10 °C using the Peltier effect, with a resolution of 165 eV at 5.9 keV. The relative geometry between the source and the detector is fixed, and the position of the analysis spot is controlled at the intersection of two lasers and a video camera connected to the whole system.

The quantitative analysis of the chemical composition of the elements detected by portable XRF (PXRF) was carried out using the programme PyMca developed in the ESRF (European Synchrotron Radiation Facility) by Solé, Papillon, Cotte and others (2007). The fundamental parameter approach was implemented utilising known composition patterns. The inclusion of the experimental parameters utilised (geometrics, conditions of acquisition and of the X-ray tube emission spectrum) allowed for the simulation of fluorescence spectra and the estimation of concentration from the adjustment areas of the chemical elements identified in each sample. With this PXRF method, the concentrations of the light elements such as Na, Al and Mg –whose low energy emission is strongly absorbed by the air and by the Be detector window– were not determined (GIANONCELLI; CASTAING; BOUQUILLON, et al., 2006), thus the reason why the concentrations were not normalised to 100%. In any case, the composition of the glazes is considered to be uniformly homogeneous.

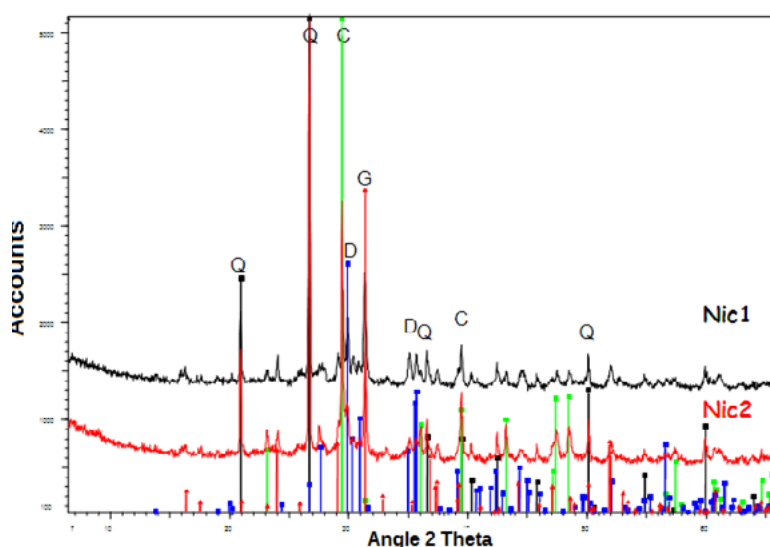
Identification of the crystalline phases in the pastes and glaze pigments was complemented by portable Raman spectroscopy using fibre-optic technology; this device incorporates a fibre-optic probe connected to a 785 nm diode laser with an emission that can be adjusted between 100 and 700 mW; the laser signal is guided by a 50  $\mu$ m-diameter optical fibre and the Raman signal is picked up by a 100  $\mu$ m-diameter fibre and led to the spectrometer. The probe head incorporates a bandpass interference filter and a focusing lens (5X increments) with a 4 cm focal length. The detector is a 1024x256 pixel CCD (from BTW) cooled by the Peltier effect. In addition to using the probe in a conventional way,

a mount has been designed which allows objectives to be adjusted to different magnification factors (between 10x and 50X), thus allowing the analysis spot to be focused and the signal –picked up by a camera connected to the system– to be observed on a laptop screen. Phase identification was conducted through comparison with Raman spectral libraries (BELL; CLARK; GIBBS, 1997; BOUCHARD; SMITH, 2003; BUZGAR; APOPEI; BUZATU, 2009).

In order to assess the chemical homogeneity of the glazes and determine their microstructure, cross sections of samples were analysed with scanning electron microscopy (SEM) using a JEOL JSM 6400 microscope featuring an energy dispersive X-ray analysis system (EDX) for the elementary analysis.

Two micro-samples from the ceramics were soaked in resin and polished perpendicularly to the surface of the glaze; this allowed for the observation of the different layers between the surface and the ceramic paste. The ZAF correction procedure was utilised for the quantification of the analyses carried out.

The data set from the  $\mu$ -XRF chemical analysis and from the PXRF spectra corresponding to the same glazes was utilised to establish a procedure that allows for the quantitative chemical characterisation (using PXRF) of other works whose analysis by means of conventional techniques is not possible. The effectiveness of this procedure was assessed by analysing a set of spectra that are characteristic of the Nic2 tile.



**Graphic 1 |**  
Diagram of X-rays in the Nic1 and Nic2 pastes. Quartz diffraction lines (Q) are represented in black, calcite (C) in green, diopside (D) in blue and gehlenite (G) in red

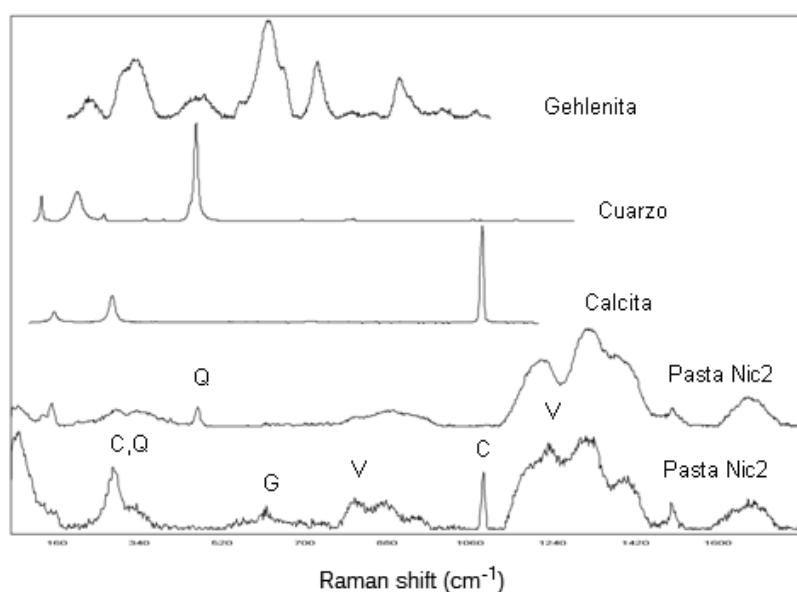
## RESULTS AND DISCUSSION

### Analysis of Pastes

The mineralogy of the ceramic pastes in tiles Nic1 and Nic2 inferred from their analysis by X-ray diffraction includes quartz, calcite, feldspars, gehlenite and diopside, wherein quartz is the major crystalline phase in both ceramics (graphic 1); we can also observe the presence of typical thermal transformation phases of calcareous clay, gehlenite and diopside to a lesser extent, as well as remnants of calcite that have not been transformed. This data allows us to conclude that the clays utilised to create both tiles are similar, and that the ceramic was fired at a relatively low temperature range (<850 °C) and/or by fast firing processes. These results are consistent with the presence of fossil remains of calcite –that have not been transformed– which can be observed under a microscope.

Some of the phases observed with XRD were identified with portable Raman spectroscopy (graphic 2); the spectra acquired for two spots on the paste of Nic2 show the band at 463  $\text{cm}^{-1}$  corresponding to quartz, bands at 1090  $\text{cm}^{-1}$  and 280  $\text{cm}^{-1}$  corresponding to calcite, the widest band at 615  $\text{cm}^{-1}$  corresponding to gehlenite, and different bands associated with the Si–O vibrational modes from the vitreous phase (V).

To complement characterisation of the pastes, a conventional chemical analysis of the major and minor elements was conducted by XRF of two powder samples representative of tiles Nic1 and Nic2, the results



**Graphic 2 |**

Raman spectra of the Nic2 paste on two different spots where the characteristic bands of crystalline phases were detected: quartz (Q), calcite (C) and gehlenite (G) whose "pattern" spectra are indicated in the corresponding spectra, as well as the different bands associated with the Si-O vibrational modes from the vitreous phase (V)

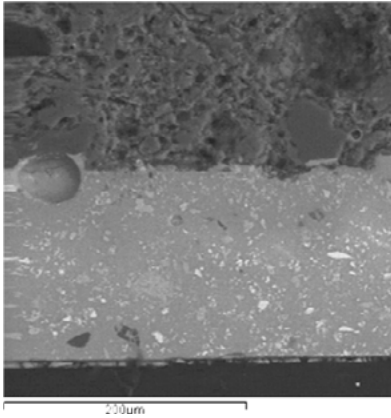


**Image 3 |**

BSEM image of the yellow glaze and the Nic2 tile paste. Quartz crystals appear in black, heterogeneous aggregates with Si-Pb-Sn and cassiterite aggregates appear in grey and the lightest tones correspond to Pb and Pb-Zn-Si antimonate crystals responsible for the glaze's yellow colour

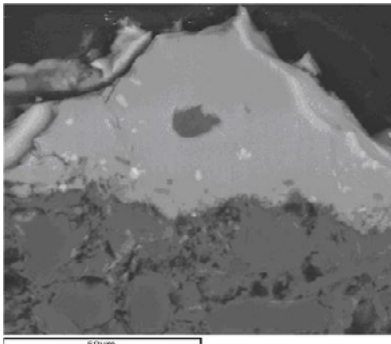


**Image 4 |**

BSEM textural details of the boundary between the white glaze (above) and the paste (below) in Nic1. Note the presence of some cassiterite aggregates shown in white and quartz crystals in dark grey

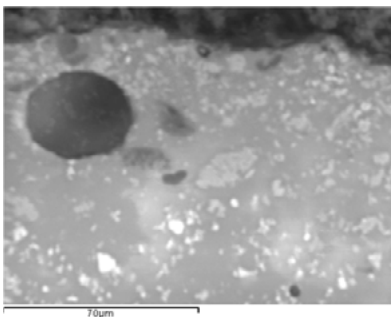


**Image 5 |**

Close-up of image 3 of the Nic2 glaze with heterogeneous aggregates with Si-Pb-Sn and crystals appearing in grey tones and Pb and Pb-Zn-Si antimonates in lighter colours

of which are indicated in table 1. In order to compare the origin of the clays utilised, the last column of the table (RFM) includes the composition ranges of the pastes utilised in the production of ceramics with lustre made in Seville during the 16th century (POLVORINOS; CASTAING, 2010), that is, during the same time period.

It is observed that the composition of the Nic1 and Nic2 ceramic pastes (table 1) matches the typical calcareous paste from the Guadalquivir Valley utilised in the manufacturing of lustre (POLVORINOS; CASTAING, 2010); the concentration ranges of all of the major and minor elements in the pastes of Pisano's tiles are close to the paste ranges of ceramics decorated with lustre, including the concentrations measured in Pisano's pieces. These results, in addition to the paste mineralogy, allow us to conclude that clays from the Guadalquivir Valley, and more specifically from the pottery district of Seville, were utilised in the production of these tiles.

### Analysis of Glazes

The study of the glazes includes the analysis by SEM-EDX of tile cross-sections, the chemical analysis by  $\mu$ -XRF and PXRF of the different colours present in the decoration of each object and the characterisation of the pigments utilised using Raman spectroscopy.

### Scanning Electron Microscopy

The results obtained in two micro-samples are presented for the structural analysis of the glazes using SEM: one micro-sample in the white glaze of tile Nic1; and another yellow micro-sample in the tile Nic2. Close-ups of the cross-sections of the Nic2 and Nic1 enamels are shown in images 3 and 4, respectively. The SEM observation of the interface reactions between the pastes and the glazes in both cases suggests that a double firing technique was utilised (TITE; FREESTONE; MASON et al., 1998; MOLERA; PRADELL; SALVADO et al., 2001; PRADELL; MOLERA; SMITH et al., 2008), the presence of bubbles in the glazes is scarce. In both enamels, whose thicknesses vary between 100 and 150 microns, the rare, undissolved quartz crystals stand out in addition to the absence of feldspars and Ca phosphate crystals; the use of calcined bone in the preparation of Pisano's enamels is ruled out, in contrast to its frequent use in the production of Renaissance enamels.

The crystals presenting the greatest difference in atomic number (presence of Pb) are concentrated in the outermost layer of the Nic2 yellow glaze, although we do not observe such a clear difference as that of the Renaissance ceramics of Derruta and Gubbio (VITI, BORGIA; BRUNETTI et al., 2003).

The detailed analyses of some aggregates with contrasts typical of intermediate atomic numbers in the Nic2 enamel (image 5) do not entirely correspond to cassiterite crystals since they present, aside from Sn, elevated levels of Si and Pb, thus indicating the presence of aggregates small cassiterite crystals in the glass matrix.

The crystals presenting a greater difference in atomic number correspond to the pigment utilised to obtain the yellow colouring; the EDX analysis of these crystals indicates that their composition is not homogeneous, as spots of Pb antimonate were measured (Naples yellow  $Pb_2Sb_2O_7$ , corresponding to 60% PbO and 40%  $Sb_2O_3$ ) as well as other spots with levels that vary in percentage (%) (0-1.0  $Na_2O$ , 0-0.9  $Al_2O_3$ , 5.4-8.3  $SiO_2$ , 0-0.5  $K_2O$ , 1.5-1.9 CaO, 0.4-0.8  $Fe_2O_3$ , 3.4-3.7 ZnO, 33.1-37.3  $Sb_2O_3$ , 47.8-52.6 PbO). Despite the fact that the indicated variability may be due to the partial contribution of the vitreous matrix for Si or Pb, the concentrations measured for ZnO suggest the presence, although limited, of Pb-Zn antimonates with a pyrochlore crystalline structure that is responsible for the yellow colour. This variability in composition is similar to the variability detected in other ceramic productions (VITI, BORGIA; BRUNETTI et al., 2003) as well as in results from experiments regarding the reproduction of this type of pigment (BULTRINI; FRAGALA; INGO et al., 2006).

Although the presence of Zn in this pigment in the Nic2 tile was not detected during the XRF analysis (micro and portable), –probably due to its presence solely in some particles of the top layer of the enamel (image 3)– its presence in the yellow of the Nic1 tile was confirmed by XRF analysis (see below, table 2). This type of yellow pigment may be isostructural with those found in glazes from Della Robbia with Sn and without Zn (DURAN; CASTAING; LEHUÉDÉ et al., 2011) and in some Italian ceramics from the 16th century (SAKELLARIOU; MILIANI; MORRESI et al., 2004; SANDALINAS; RUIZ-MORENO; LÓPEZ-GIL et al., 2006). The presence of Pb-Zn pyroantimonates was not identified in maiolica enamels (PADELETTI; FERMO; BOUQUILLON et al., 2010); an enamel with 0.3% ZnO and 1%  $Sb_2O_5$  was only found in a ceramic object (PADELETTI; IGNO; BOUQUILLON et al., 2006), although it was determined that it was used as a pictorial pigment (HRADIL; GRYGAR; HRADILOVÁ et al., 2007).

Despite the fact that the first observation that the use of Zn in Pb-Sb yellow enamels was recently reasserted (ROSI; MANUALI; MILIANI et al., 2011), the likely use of Pb-Zn antimonates in Pisano's ceramic decoration has been confirmed. The Pb-Sb-Zn composition of the yellow utilised by Pisano in the Nic1 tile suggests that ZnO “tuttia alexandrina” was used in its production (DIK; HERMENS; PESCHAR et al., 2005).

### X-ray microfluorescence ( $\mu$ -XRF), portable X-Ray Fluorescence (PXRF) and portable Raman spectroscopy

One of the objectives of this study was to compare the usefulness of standard qualitative data from PXRF with the quantitative results from  $\mu$ -XRF obtained in the same analysis spots. The dual purpose of this study consists in, first of all, determining –for the first time– the composition ranges of the glazes, produced in Seville by the Italian artist with an extensive and valuable ceramic collection, by conducting a non-destructive  $\mu$ -XRF analysis; secondly, the study assesses and models the PXRF data for the non-destructive quantitative analysis of ceramic pieces that can not be taken to a laboratory for analysis using conventional methods as a result of their location and/or artistic value. To do so, the calculation models of element concentrations were adjusted using the  $\mu$ -XRF quantitative analyses and the calculations of PXRF peak areas; the calculations for the different chemical elements were carried out from the spots indicated in images 1 and 2.

Furthermore, a preliminary assessment is presented regarding the use of the portable Raman technique for identification, where appropriate, of the phases responsible for the colouring in the glazes.

	XRF1 Green	XRF2 White	XRF3 Blue	XRF5 Yellow	XRF4 Brown
Na <sub>2</sub> O	0.50	0.59	1.82	1.10	
MgO					
Al <sub>2</sub> O <sub>3</sub>		0.53			
SiO <sub>2</sub>	44.44	48.41	52.25	56.00	59.31
SO <sub>3</sub>					
K <sub>2</sub> O	1.65	1.96	5.32	3.85	4.37
Sb <sub>2</sub> O <sub>3</sub>				2.43	
CaO	3.94	5.92	6.11	4.24	7.07
TiO <sub>2</sub>	0.13	0.08	0.12	0.10	0.19
V <sub>2</sub> O <sub>5</sub>	0.02		0.01	0.05	0.01
Cr <sub>2</sub> O <sub>3</sub>	0.02	0.01	0.03	0.05	0.02
MnO	0.05	0.04	0.16	0.05	0.80
Fe <sub>2</sub> O <sub>3</sub>	0.78	0.91	0.99	0.71	0.88
CoO	0.01		0.51	0.01	0.03
Ni <sub>2</sub> O <sub>3</sub>	0.02		0.13	0.02	0.01
CuO	3.40	0.11	0.08	0.09	0.10
ZnO	0.02	0.02	0.04	3.5	0.02
As <sub>2</sub> O <sub>3</sub>	0.78	0.65	0.77	0.64	0.65
PbO <sub>2</sub>	24.72	25.58	25.04	24.48	23.80
SrO	0.11	0.10	0.08	0.09	0.08
SnO <sub>2</sub>	3.90	2.76	3.52	2.59	2.64

**Table 2 |**  
 $\mu$ -XRF (% mass) of the colours of Nic1 (XRF1 to 5)

The analytical data for the different colours studied with  $\mu$ -XRF in the Nic1 tile is indicated in table 2; the data for the Nic2 tile is indicated in the first column of each colour in table 3. The calculation –using PXRF spectra– of the chemical composition of the elements in the Nic2 glazes is shown for each colour in the corresponding column in table 3, preceded by the concentration data measured for the same spots using  $\mu$ -XRF.

In order to compare the  $\mu$ -XRF and PXRF methods, we must first bear in mind that the  $\mu$ -XRF measurements were taken using a 50  $\mu$ m-diameter probe, while the diameter of the PXRF X-ray beam measures 2 mm; thus, local concentration variations are expected with each analysis method. Secondly, the effects of absorption of fluorescence radiation at low energies differ substantially between the two methods, as the absorption by air in PXRF will be greater than the absorption that takes place in the vacuum chamber of the  $\mu$ -XRF analyser. As a result of the absorption of the layer of air, the PXRF technique prevents reproducible data from being obtained for the elements Na, Mg and Al; for Si ( $E=1.7\text{keV}$ ), the results are somewhat dispersed (table 3) due to the fact that the thickness of the air which the X-rays pass through is not perfectly controlled.

For higher energies, the quality of the PXRF data is not affected by the air, although other problems can arise if the top layer of the ceramic has been modified by alteration processes caused by the environment in which it was buried for centuries; under these conditions the composition may not be homogeneous throughout all of the enamel. In these cases, the method for calculating the concentrations will depend on the type of XRF line utilised. Hence, for instance, for Sn-K or Sb-K ( $\approx 25\text{keV}$ ) X-ray penetration is on the order of 120  $\mu$ m, and 5  $\mu$ m for Sn-L and Sb-L ( $\approx 4\text{keV}$ ); while the radiation would cover most of the thickness of the glaze in the first case, it would only penetrate the top layer in the second case (images 3 and 5). For the PXRF the Sn-L line was utilised, meaning that the results would correspond to the top layer, thin with regard to the thickness of the glazes (images 3-5).

Another type of problem arises with the determination of As, whose most intense peak ( $\text{As-K}\alpha$ ) coincides with an intense Pb-L line (10.5 keV). In a material rich in Pb, as is the case with our glazes, it is difficult to obtain a good estimation of the concentration of arsenic from  $\text{As-K}\alpha$  and it would be better to utilise the  $\text{As-K}\beta$  line (11.7 keV) isolated in the XRF spectrum. While the concentration calculation details are not available with the commercial  $\mu$ -XRF analyser from CITIUS at the University of Seville, the fluorescence lines to be used in the calculations can be chosen with the PXRF technique. Consequently, in certain cases, the differences between  $\mu$ -XRF and

PXRF can indicate this type of problem. Thus with  $\mu$ -XRF, for example, concentrations between 0.5 and 0.8%  $\text{As}_2\text{O}_3$  (tables 2 and 3) have been estimated, and with the PXRF technique they are not detected; in other words, the latter gives concentrations that are null in all cases except for brown (table 3).

In general it is observed that the concentrations of K, Ca, Pb and Sn by PXRF underestimate the measurements given with  $\mu$ -XRF, although the estimated and measured composition ranges are similar in all cases; in spite of the absolute differences in the estimations of Pb, the concentrations obtained using the L and M lines of Pb are similar. With regard to the specific elements in the pigments, composition ranges that are compatible with the nature of each pigment have been estimated in all cases despite the expected variability inherent in the experimental differences between the two methods and the heterogeneity of their spatial distribution.

**Table 3 |**

Estimation by the Fundamental Parameter approach of the composition in % oxides in the Nic2 glazes from the  $\mu$ -XRF and PXRF spectra (XRF6 to XRF11; see spots in image 2)

The white enamels in both tiles define the basic composition of the glaze (26%  $\text{PbO}_2$  –table 2– and 21%  $\text{PbO}_2$  –table 3–, according to the  $\mu$ -XRF). The enamels in both tiles are plumbo-calco-alkalines mainly

	Green		White		Blue		Yellow		Brown		Beige	
	XRF11	PXRF	XRF9	PXRF	XRF8	PXRF	XRF6	PXRF	XRF10	PXRF	XRF7	PXRF
$\text{Na}_2\text{O}$	1.22		0.71		1.01		2.16				0.72	
$\text{MgO}$												
$\text{Al}_2\text{O}_3$		2.3		2.97	3.59	2.27		3.78		2.82		3.60
$\text{SiO}_2$	63.75	73.0	66.43	66.99	62.69	68.66	66.42	65.87	60.86	86.21	61.78	53.00
$\text{SO}_3$		0.0		0.00	0.74	0.00	0.00	0.00		0.73		0.00
$\text{K}_2\text{O}$	6.18	5.6	5.30	4.29	6.01	5.18	5.42	4.58	6.43	6.16	6.13	5.42
$\text{CaO}$	4.7	3.1	3.83	2.66	4.26	2.94	2.81	2.80	4.08	3.44	2.98	2.80
$\text{TiO}_2$	0.12	0.2	0.16	0.17	0.15	0.17	0.09	0.17	0.14	0.20	0.09	0.17
$\text{V}_2\text{O}_5$	0.03	0.0	0.01	0.07		0.00	0	0.00		0.02	0.01	0.00
$\text{Cr}_2\text{O}_3$	0.02	0.0	0.02	0.02	0.01	0.00	0.03	0.00	0.02	0.01	0.01	0.00
$\text{MnO}$	0.05	0.1	0.03	0.02	0.32	0.16	0.01	0.00	2.85	0.46	0.02	0.00
$\text{Fe}_2\text{O}_3$	1.9	1.3	0.46	0.34	3.32	1.29	0.95	0.57	4.20	1.77	4.22	2.72
$\text{CoO}$	0.21	1.3	0.01	0.00	0.70	0.89	0.01	0.00	0.06	1.92	0.02	0.13
$\text{Ni}_2\text{O}_3$	0.1	0.1		0.01	0.49	0.14	0.03	0.00	0.03	0.18	0.01	0.00
$\text{CuO}$	0.96	0.6	0.19	0.11	0.12	0.13	0.08	0.13	0.22	0.16	0.12	0.13
$\text{ZnO}$	0.32	0.2	0.02	0.00	0.02	0.00	0.02	0.00	0.02	0.00	0.01	0.00
$\text{As}_2\text{O}_3$	0.54	0.1	0.52	0.00	0.56	0.00	0.13	0.00	0.53	1.14	0.24	0.00
$\text{SrO}$	0.1	0.1	0.08	0.07	0.06	0.12	0.09	0.00	0.07	0.02	0.07	0.12
$\text{SnO}_2$	1.45	1.8	1.57	1.22	1.3	1.65	1.27	1.40	1.63	1.96	1.11	1.40
$\text{Sb}_2\text{O}_3$	0.09	0.2		0.01		0.21	2.98	0.96		0.10	2.49	2.13
$\text{PbO}_2\text{L}$	18.4	15.0	20.64	15.04	14.56	14.43	17.53	15.58	18.84	17.70	19.98	12.70
$\text{PbO}_2\text{M}$		13.2		13.77		12.93		14.43		17.86		11.43

composed of Pb and Si. The flux is similar in both tiles; a slight increase in Pb is detected in the Nic1 tile (average of 25%  $\text{PbO}_2$ ) compared to the Nic2 tile (15-21 %  $\text{PbO}_2$ ); an inverse variation in the level of K is detected with 3 %  $\text{K}_2\text{O}$  in Nic1 compared to 6 %  $\text{K}_2\text{O}$  in the Nic2 tile. Sn was utilised as an opacifier in both tiles and it was observed that the concentrations in the top layer of the Nic1 tile are somewhat higher (3.4%  $\text{SnO}_2$ ) than in Nic2 (1.5 %  $\text{SnO}_2$ ). These concentration ranges for  $\text{SnO}_2$  are closer to those of the ceramics with lustre from Mastro Giorgio (PADELETTI; IGNO; BOUQUILLON et al., 2006) than to the high concentrations in Della Robbia production (GIANONCELLI; CASTAING; BOUQUILLON et al., 2006; ZUCCHIATTI; BOUQUILLON, 2011).

The white glazes utilised in the ceramics with lustre produced in Seville (POLVORINOS; CASTAING, 2010) present concentrations of  $\text{PbO}_2$  ( $33.5 \pm 3.6$ ) and  $\text{SnO}_2$  ( $8 \pm 1.26$ ) greater than that of the white glazes found in Pisano's collection; nevertheless, the concentrations of  $\text{K}_2\text{O}$  ( $4.1 \pm 1.05$ ) and  $\text{CaO}$  ( $2.8 \pm 0.87$ ) are similar. It should be pointed out that  $\text{Fe}_2\text{O}_3$  levels are less than 1% in the XRF2 (table 2) and XRF9 (table 3) white spots, thus indicating that the silica sand used to make the enamels was very pure; the latter is also confirmed by the absence of phase inclusions such as feldspars in the enamels.

The composition of the yellow glazes in both tiles determined by  $\mu$ -XRF is characterised by high concentrations of Sb (2.5-3%), thus indicating the use of Pb antimonate (Naples yellow), as this pigment is well known and has been utilised since Antiquity (DIK; HERMENS; PESCHAR et al., 2005; VIGUERIE; DURAN; BOUQUILLON et al., 2009). The presence of ZnO in the Nic1 tile is significant and characteristic (spot XRF5 in table 2) given that this element is not detected in the composition of the yellow glaze in the second tile, based on lead antimonate (spot XRF6 in table 3); however, we must take note that the Zn detection limit in XRF is high in these glazes due to the presence of several lines close to those of Zn (graphic 3). As we previously mentioned, the concentration of Sb according to PXRF corresponds to a layer on the order of 5  $\mu\text{m}$  where pigments of the type Pb-Sb-X-O (X= Fe, Sn, Si, Zn) were detected.

The X-ray microdiffraction ( $\mu$ -XRD) analysis of the yellow (Nic1 and Nic2) and beige (Nic2) pigments confirmed the presence of cubic pyrochlore phases in all cases; the X-ray diagram of the Nic2 yellow matches up with the diffraction lines of synthetic bindheimite  $\text{Pb}_2\text{Sb}_2\text{O}_7$  (PDF file 1-074-1354, with cell parameter of  $a=1.040$  nm), thus confirming that it is likely Naples yellow; the substitution of Zn in the yellow of Nic1 and of Fe in the beige of Nic2 is manifested by a slight increase in the size of the cells (1.0456 nm and 1.0421 nm respectively). These results are consistent with the small increases in

cell size of the pyrochlore structure caused by the substitution of these elements in octahedral coordination (ROSI; MANUALI; MALINI et al., 2009).

The results indicated highlight the fact that Pisano's ceramic production included various types of yellows from synthesised lead antimonates. This initial observation coincides with the Renaissance practice of producing Naples yellows modified by the addition of Sn, Zn and Si, something which has been the subject of several investigations on the use of lead pyroantimonates in 16th century Italian maiolica and other Spanish ceramic production centres (DIK; HERMENS; PESCHAR et al., 2005; ROSI; MANUALI; MALINI et al., 2009; FERRER; RUIZ-MORENO; LÓPEZ-GIL et al., 2001; ROSI; MANUALI; GRYGAR et al., 2011).

The PXRF spectra for the yellow enamel in the Nic1 and Nic2 tiles (graphic 3) reflect the compositional difference indicated by the  $\mu$ -XRF analyses (tables 2 and 3), although the estimation of Sb levels with PXRF for Nic2 is lower than the estimation from  $\mu$ -XRF (table 3).

Graphic 4 shows the Raman spectra characteristic of the yellow pigments as well as the position of the bands; given the compositional proximity of the colour beige which only appears in Nic2 (table 3), its characteristic Raman spectrum is also included in Graphic 4. In no case were the bands characteristic of cassiterite identified; these were not detected by XRD until some 20  $\mu$ m from the surface (penetration of X-rays) despite concentrations of Sn between 1 and 4% in the top layer. The Raman spectrum for Nic1, the tile in which Zn was identified in its chemical composition, presents features similar to those described for Pb pyroantimonate modified with Zn; the absence of the band at 510  $\text{cm}^{-1}$  (A1g mode) and the displacement of the band Pb-O at 143  $\text{cm}^{-1}$  on the Nic1 tile match the observations described by Rosi, Manuali, Grygar and others (2011). On the Nic2 spectrum (graphic 4), the A1g mode corresponding to the symmetrical elongation of the octahedrons  $\text{SbO}_6$  at 510  $\text{cm}^{-1}$  was detected in addition to the absence of bands at 450  $\text{cm}^{-1}$ , characteristic of the non-modified structure of Pb antimonate. The presence of rosiaite (hexagonal form of  $\text{PbSb}_2\text{O}_6$ ), identified by its main band at 665  $\text{cm}^{-1}$ , and its association with the synthesis of pyroantimonates from non-stoichiometric proportions of Pb:Sb would indicate that it is likely a non-modified Pb antimonate but with a non-stoichiometric proportion of Pb:Sb.

In addition to the presence of Sb in the beige enamel of the Nic2 tile, the elevated concentration of  $\text{Fe}_2\text{O}_3$  (3-4 %) stands out as being responsible for the change in colour, both measured by  $\mu$ -XRF and estimated by PXRF (table 3). This observation is similar to that presented by the Pb antimonate crystals in Derruta and Gubbio ceramics (VITI, BORGIA;

BRUNETTI et al., 2003); this concentration of Fe was deliberate with the aim of modifying the Naples yellow for a beige tone.

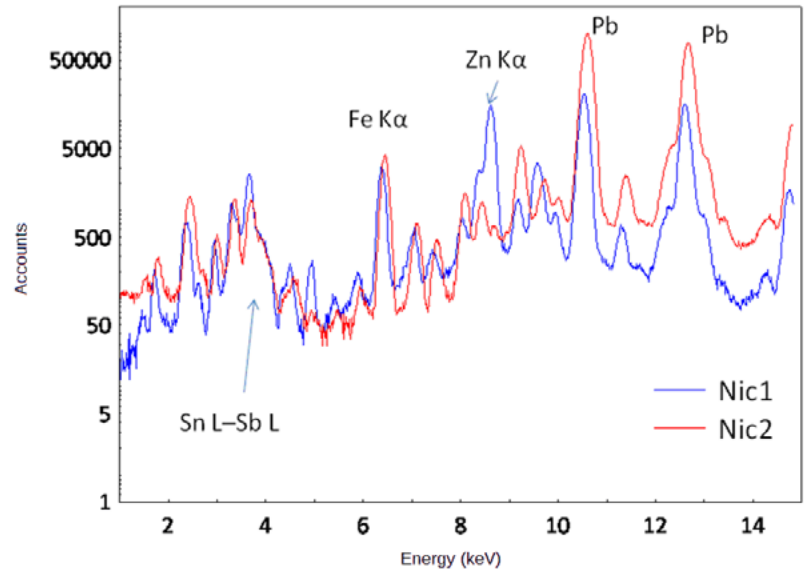
Its Raman spectrum is well identified (graphic 4) with the bands characteristic of a Pb antimonate, which with regard to yellow, present the relatively less intense band at  $510\text{ cm}^{-1}$  and a 128-143 doublet of Pb-O; the band at  $660\text{ cm}^{-1}$ , assigned to rosiaite, which in the Nic2 yellow was intense, is very weak in the beige spectrum; conversely, the bands at  $300$  and  $330\text{ cm}^{-1}$  appear to be better identified than in the yellow spectrum. These spectral characteristics are similar to those observed in Pb pyroantimonates doped with Zn, Sn and Si; in the case of our pigment, these structural modifications may be due to the substitution of Fe which, if confirmed, would indicate the capacity of this ceramist to create pigments from Pb antimonates modified by the addition of Fe and Zn, just as suggested by the variability in the compositions of the yellows found. We did not detect the use of other phases such as Fe oxides mixed with Naples yellow; this would have allowed us to justify the tone of this pigment.

Although the green enamels in both tiles incorporate Cu (3.4% CuO in Nic1 and 1% in Nic2), the composition of the pigment utilised in each tile is different (tables 2 and 3). A significant concentration of Zn (0.2-0.3% ZnO) is observed in the composition of the Nic2 tile, while it is absent from the composition of Nic1. The identification of Co in the Nic2 green indicates the possible application of a mix of blue enamel and iron (2%  $\text{Fe}_2\text{O}_3$ ) to obtain the tone desired by the artist (see table 3).

The  $\mu$ -XRF analyses of the blue enamels in both tiles correspond to glazes with Co as a chromophore element, as well as the presence of Ni by geochemical association in the Co-Ni-Fe-As ores utilised (tables 2 and 3). The results correspond to the typical zaffre obtained by roasting complex Co or Ni arsenides and sulfoarsenides, such as skutterudite  $\text{CoAs}_3$ , erythrite  $[\text{Co,Ni}]_3[\text{AsO}_4]_2 \cdot 8\text{H}_2\text{O}$ , safflorite  $[\text{Co,Ni}]\text{As}_2$ , cobaltite  $\text{CoAsS}$ , etc., a process during which the volatilisation of As can occur (GRATUZE; SOULIER; BLET et al., 1996; PADELETTI; IGNO; BOUQUILLON et al., 2006; ZUCCHIATTI; BOUQUILLON; KATONA et al., 2006). However, the composition of mix of the minerals used to obtain the enamels utilised in each case are different: the Fe concentration of the Nic2 enamel (3.3%  $\text{Fe}_2\text{O}_3$ ) is significantly greater than the concentration of its white glaze (0.46%  $\text{Fe}_2\text{O}_3$ ); meanwhile, the Nic1 tile presents similar concentrations (0.99-0.91%  $\text{Fe}_2\text{O}_3$ ), thus suggesting the use of a product with fewer impurities and therefore making it richer in Co. The high  $\text{SO}_3$  and  $\text{Al}_2\text{O}_3$  concentrations in the blue enamel of Nic2, as well as the elevated NiO/CoO relationship in this enamel, suggest a pigment preparation whose Co level was less concentrated than that of Nic1, whose Ni/Co relationship is 0.5.

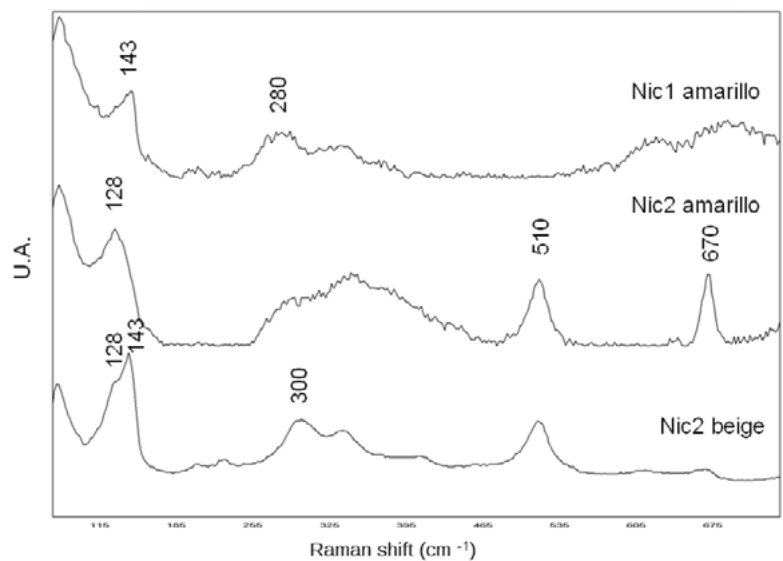
### Graphic 3 |

PXRF spectrum of the yellow enamel in the Nic1 and Nic2 tiles where Sb-L, Sn-L and Pb-L are detected, thus suggesting the presence of Pb antimonate (Naples yellow,  $Pb_2Sb_2O_7$ ) in both cases; the abundance of Zn in the composition of Nic1 contrasts with its near absence in the Nic2 tile, indicating the presence of Pb-Zn pyroantimonates in the top layer of Nic1. The spectra have been slightly shifted in order to visualise their differences



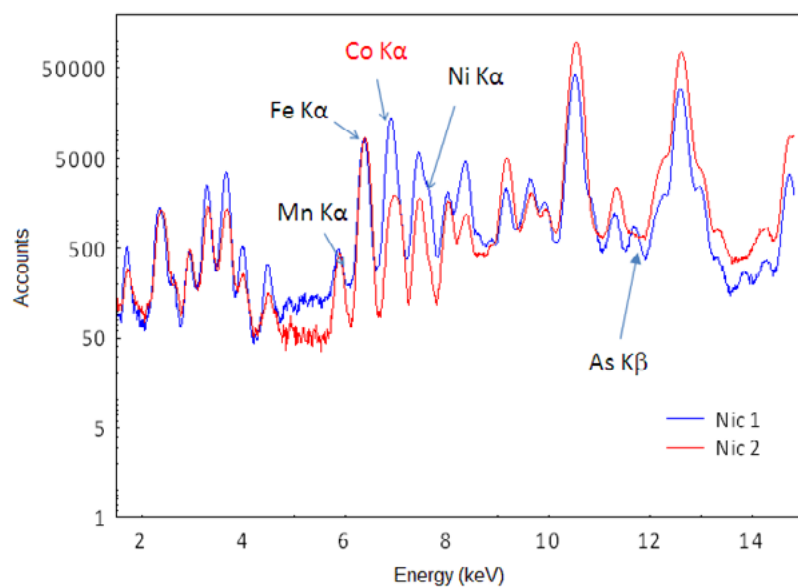
### Graphic 4 |

Raman spectra characteristic of the yellow enamels in the Nic1 and Nic2 tiles, and of the beige which is only present in Nic2

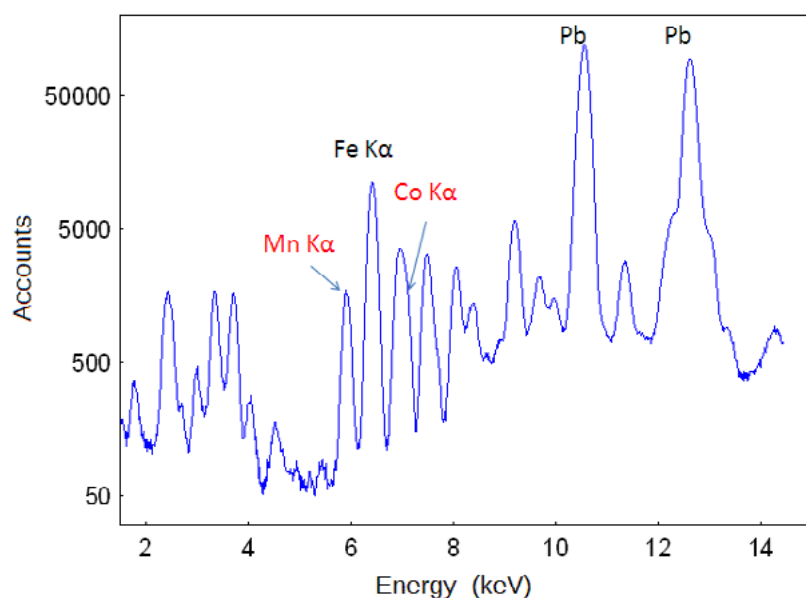


Differences are evident in the PXRF spectra, in which the absence of As in the Nic2 spectrum (graphic 5; table 3) stands out, likely due to its volatilisation, in addition to the presence of a low concentration in Nic1.

The presence of Mn, likely incorporated as Mn-Fe oxides in order to obtain the brown enamel, is characteristic of both tiles (tables 2 and 3), though presenting different concentration ranges which are



**Graphic 5 |**  
 PXRF spectra of the blue enamels in the Nic1 and Nic2 ceramics



**Graphic 6 |**  
 Portable XRF spectrum of the dark brown enamel of the Nic2 tile in which we can observe the addition of blue enamel based on Co-Ni

higher in the Nic2 tile (4.2%  $\text{Fe}_2\text{O}_3$  and 2.85% MnO) than in the Nic1 tile (0.88%  $\text{Fe}_2\text{O}_3$  and 0.8% MnO); the Fe concentration of the Nic2 glaze (4.2%  $\text{Fe}_2\text{O}_3$ ) is significantly higher than that of the white glaze (0.46%  $\text{Fe}_2\text{O}_3$ ).

Meanwhile, these concentrations are similar in the Nic1 tile (0.88-0.91%  $\text{Fe}_2\text{O}_3$ ) which indicates that Mn oxides were utilised in the Nic1 tile whereas a mix of Mn and Fe oxides was used for the Nic2 tile.

Another example of the use of a mix of pigments or their simple juxtaposition in order to obtain the colour levels observed in the Nic2 tile was detected in the darkest of browns. A PXRf spectrum which is representative of this practice is shown in graphic 6, where we can observe the association among Fe, Mn, Co and Ni, thus suggesting the application of brown and blue enamels in the same spot.

## CONCLUSIONS

The ceramics of Niculoso Pisano that we have analysed have allowed us to verify their specific production characteristics, particularly with regard to the type of pigments utilised in decoration. Despite the limited palette of basic colours, the mix of pigments and their dilution generate a certain diversity of colour that is rare in the field of ceramics and contrasts with other productions.

Although only two tiles were analysed, the basic aspects of the ceramics are similar, both in the relatively simple preparation of the surface –normalised when decorated– and in a certain consistency among the glaze compositions which are based on opacified Pb-K-Ca with low SnO<sub>2</sub> concentrations.

The greatest diversity in the nature and composition of the tiles can be observed in the pigments.

The composition of some of the pigments in the two tiles is different. In some cases these differences are due to changes in the composition of the minerals utilised, while in others they are the result of the production processes; thus, the differences in the Co/Ni relationship in the blues based on Co suggest a certain change in the raw minerals, something which can be a parameter for the relative dating of undated productions.

In the elaboration of the yellow and beige enamels, Pisano's ceramics have a distinct specialisation which has not been observed to date in other ceramic productions from the same time period. Only two types of yellow enamels based on Pb antimonates were found in the two tiles studied: one Naples yellow, and another modified by the addition of Zn and whose characterisation was conducted, both in terms of level of chemical composition and phase identification, by Raman spectroscopy; the incorporation of Fe with Pb antimonates in order to obtain the beige pigments on Pisano's palette was also demonstrated. A lack of models concerning documentation of the systematic use of these types of compounds modified with Zn and Fe means that an exhaustive analysis of Pisano's ceramic production is the focus of a study that is still in progress.

We can observe that Pisano's palette includes, in addition to the conventional pigments found in other ceramic productions from Italy and Spain, other more specific pigments which indicate a deep knowledge of enamel preparation techniques –closely connected to glass production– which was likely brought to Spain from Italy though the details of his activity before moving to Seville are unknown.

It has been shown that the combined use of PXRF and portable Raman techniques makes it possible to overcome their individual limitations in order to approach the characterisation of the materials in works of art; the PXRF analysis method has been proven viable for the quantitative analysis of the chemical composition of the enamels, and thus useful for the in situ analysis of other ceramic works; phase characterisation with a sufficient Raman signal, even under relatively intense fluorescence conditions, has proven crucial to differentiating between some of the most interesting pigments in Pisano's production.

#### **Acknowledgements**

The authors express their appreciation for the attention received from the General Research Services of the University of Seville (CITIUS) technical team over the course of this study.

## BIBLIOGRAPHY

- BELL, I. M.; CLARK, R. J. H.; GIBBS, P. J.** (1997)  
 Raman spectroscopic library of natural and synthetic pigments (pre- ≈ 1850 AD). *Spectrochimica Acta Part A: Molecular and Biomolecular Spectroscopy*, October 1997, vol. 53, issue 12, pp. 2159-2179
- BOUCHARD, M.; SMITH, D. C.** (2003)  
 Catalogue of 45 reference Raman spectra of minerals concerning research in art history or archaeology, especially on corroded metals and coloured glass *Spectrochimica Acta Part A: Molecular and Biomolecular Spectroscopy*, August 2003, vol. 59, issue 10, pp. 2247-2266
- BULTRINI, G.; FRAGALA, I.; INGO G. M. et al.** (2006)  
 Characterisation and reproduction of yellow pigments used in central Italy for decorating ceramics during Renaissance. En *Applied Physics A. Materials Sciences and Processing*, 2006, vol. 83, pp. 557- 565
- BUZGAR, N.; APOPEI, A. I.; BUZATU, A.** (2009)  
*Romanian Database of Raman Spectroscopy* [En línea] <<http://rdrs.uaic.ro>> [Consulta: 14/10/2013]
- DAVILLIER, J. C.** (1865)  
 Niculoso Francisco, peintre céramiste italien, établi à Séville (1503-1508). En *Gazette des Beaux Arts*, marzo 1865, París, tomo XVIII, pp. 217-228
- DIK, J.; HERMENS, E.; PESCHAR, R.; SCHENK, H.** (2005)  
 Early production recipes for lead antimoniate yellow in italian art. *Archaeometry*, August 2005, vol. 47, issue 3, pp. 593-607
- DURAN, A.; CASTAING, J.; LEHUÉDÉ, P. et al.** (2011)  
 Les pigments jaunes des glaçures de l'atelier Della Robbia. En ZUCCHIATTI A.; BOUQUILLON A.; BORMAND M. (dir.) *Della Robbia. Dieci anni di Studi – Dix ans d'études*. Génova: Sagep, 2011, pp. 44-49
- FERRER, P.; RUIZ-MORENO, S.; LÓPEZ-GIL, A. et al.** (2012)  
 New results in the characterization by Raman spectroscopy of yellow pigments used in ceramic artworks of the 16th and 17th centuries. *Journal of Raman Spectroscopy*, November 2012, vol. 43, issue 11, pp. 1805-1810
- GESTOSO Y PÉREZ, J.** (1903)  
*Historia de los barros vidriados sevillanos desde sus orígenes hasta nuestros días*. Sevilla: Tipografía La Andalucía Moderna, 1903, pp. 167-218
- GIANONCELLI, A., CASTAING, J., BOUQUILLON, A. et al.** (2006)  
 Quantitative elemental analysis of Della Robbia glazes with a portable XRF spectrometer and its comparison with PIXE methods. *X-ray Spectrometry*, November/December 2006, vol. 35, issue 6, pp. 365-369
- GRATUZE, B.; SOULIER, I.; BLET, M. et al.** (1996)  
 De l'origine du cobalt: du verre à la céramique. *Revue d'Archéométrie*, 1996, vol. 20, pp. 77-94
- HRADIL, D.; GRYGAR, T.; HRADILOVÁ, J. et al.** (2007)  
 Microanalytical identification of Pb-Sb-Sn yellow pigment in historical European paintings and its differentiation from lead tin and Naples yellows. *Journal of Cultural Heritage*, 2007, vol. 8, issue 4, pp. 377-386
- LORENZO, J.; VERA, M.; ESCUDERO, J.** (1990)  
 Intervención arqueológica en la calle Pureza, número 44 de Sevilla. *Anuario Arqueológico de Andalucía 1987. Actividades de Urgencia, Informes y Memorias*, tomo III, Sevilla: Consejería de Cultura. Junta de Andalucía, 1990, pp. 574-580
- MOLERA, J.; PRADELL, T.; SALVADO, N. et al.** (2001)  
 Interactions between clay bodies and lead glazes. *Journal of the American Ceramic Society*, vol. 84, pp. 1120-1128
- MORALES MARTINEZ, A. J.** (1977)  
*Francisco Niculoso Pisano*. Sevilla: Diputación Provincial de Sevilla, 1977 (Colección Arte Hispalense, nº 14)
- PADELETTI, G.; INGO, G. M.; BOUQUILLON, A. et al.** (2006)  
 First-time observation of Mastro Giorgio masterpieces by means of non-destructive techniques. *Applied Physics A*, 2006, vol. 83, pp. 475-483
- PADELETTI G.; FERMO P.; BOUQUILLON A. et al.** (2010)  
 A new light on a first example of lustred majolica in Italy. *Applied Physics A*, 2010, vol. 100, pp. 747-761
- PLEGUEZUELO, A.** (1992)  
 Francisco Niculoso Pisano: datos arqueológicos. *Bolletino del Museo Internazionale di Faenza*, 1992, Annata LXXVIII, vol. 3-4, pp. 171-191
- PLEGUEZUELO, A.** (2009)  
 Diez preguntas sobre un azulejo: una nueva obra de Niculoso. *Butletí Informatiu de Ceràmica*, 2009, vol. 100, pp. 130-143

- PLEGUEZUELO A.** (2012)  
Niculoso Francisco Pisano y el Real Alcázar de Sevilla. *Apuntes del Real Alcázar de Sevilla*, vol. 13, Sevilla: Patronato del Real Alcázar y de la Casa Consistorial, 2012, pp. 138-157
- POLVORINOS, A.; AUCOUTURIER M.; BOUQUILLON, A. et al.** (2011)  
The evolution of lustre ceramics from Manises (Valencia, Spain) between the 14th and 18th centuries. *Archaeometry*, June 2011, vol. 53, issue 3, pp. 490–509
- POLVORINOS, A.; CASTAING, J.** (2010)  
Lustre-decorated ceramics from a 15th to 16th century production in Seville. *Archaeometry*, February 2010, vol. 52, issue 1, pp. 83-98
- PRADELL, T.; MOLERA, J.; SMITH, A. S. et al.** (2008)  
Early Islamic lustre from Egypt, Syria and Iran (10th to 13th century AD). *Journal of Archaeological Science*, vol. 35, pp. 2649-2662
- RAY, A.** (1991)  
Francisco Niculoso, called Pisano. En TIMOTHY WILSON (dir.) *Italian Renaissance pottery*. Londres, 1991, pp. 261-266
- ROSI, F.; MANUALI, V.; GRYGAR, T. et al.** (2011)  
Raman scattering features of lead pyroantimonate compounds: implication for the non-invasive identification of yellow pigments on ancient ceramics. Part II. In situ characterisation of Renaissance plates by portable micro-Raman and XRF studies. *Journal of Raman Spectroscopy*, March 2011, vol. 42, issue 3, pp. 407-414
- ROSI, F.; MANUALI, V.; MILIANI, C. et al.** (2009)  
Raman scattering features of lead pyroantimonate compounds. Part I: XRD and Raman characterization of  $Pb_2Sb_2O_7$  doped with tin and zinc. *Journal of Raman Spectroscopy*, January 2009, vol. 40, issue 1, pp. 107-111
- SAKELLARIOU, K.; MILIANI, C.; MORRESI, A. et al.** (2004)  
Spectroscopic investigation of yellow majolica glazes. *Journal of Raman Spectroscopy*, January 2004, vol. 35, issue 1, pp. 61-67
- SANDALINAS, C.; RUIZ-MORENO, S.; LÓPEZ-GIL, A. et al.** (2006)  
Experimental confirmation by Raman spectroscopy of a Pb-Sn-Sb triple oxide yellow pigment in sixteenth-century Italian pottery. *Journal of Raman Spectroscopy*, October 2006, vol. 37, issue 10, pp. 1146-1153
- SENDOVA, M.; ZHELYASKOV, V.; SCALERA, M. et al.** (2007)  
Micro-Raman Spectroscopy characterization of Della Robbia glazes. *Archaeometry*, November 2007, vol. 49, issue 4, pp. 655-664
- SOLÉ, V. A.; PAPILLON, E.; COTTE, M. et al.** (2007)  
A multiplatform code for the analysis of energy dispersive X-ray fluorescence spectra. *Spectrochimica Acta Part B*, vol. 62, pp. 63-68
- TITE, M. S.; FREESTONE, I.; MASON, R. et al.** (1998)  
Lead glazes in antiquity. Methods of production and reasons for use. *Archaeometry*, August 1998, vol. 40, issue 2, pp. 241-260.
- VIGUERIE, L. DE; DURAN, A.; BOUQUILLON, A. et al.** (2009)  
Quantitative X-ray fluorescence analysis of an Egyptian faience pendant and comparison with PIXE. *Analytical & Bioanalytical Chemistry*; December 2009, vol. 395, issue 7, pp. 2219-2225
- VITI, C.; BORGIA, I.; BRUNETTI, B. et al.** (2003)  
Microtexture and microchemistry of glaze and pigments in Italian Renaissance pottery from Gubbio and Deruta. *Journal of Cultural Heritage*, vol. 4, pp. 199-210
- ZUCCHIATTI, A.; BOUQUILLON, A.; KATONA, I. et al.** (2006)  
The Della Robbia blue: a case study for the use of cobalt pigments in ceramics during the Italian Renaissance. *Archaeometry*, February 2006, vol. 48, issue 1, pp. 131-52
- ZUCCHIATTI, A.; BOUQUILLON, A.** (2011)  
Les glaçures : atout maître des Della Robbia. En ZUCCHIATTI, A.; BOUQUILLON, A.; BORMAND M. (dir.) *Della Robbia. Dieci anni di Studi – Dix ans d'études*. Génova: Sagep, 2011, pp. 32-43